

Synthesis of a BODIPY Library and Its Application to the Development of Live Cell Glucagon Imaging Probe

Jun-Seok Lee,^{†,‡} Nam-young Kang,[‡] Yun Kyung Kim,^{†,‡} Animesh Samanta,[‡] Suihan Feng,^{‡,§} Hyeong Kyu Kim,[‡] Marc Vendrell,[‡] Jung Hwan Park,[‡] and Young-Tae Chang^{*,‡,§,‡}

Department of Chemistry, New York University, New York, New York 10003, Department of Chemistry, MedChem Program of Life Sciences Institute, National University of Singapore, Singapore 117543, Laboratory of Bioimaging Probe Development, Singapore Bioimaging Consortium, Agency for Science, Technology and Research (ASTAR), Biopolis, Singapore 138667

Received February 14, 2009; E-mail: chmcyt@nus.edu.sg

Abstract: The first BODIPY library (**BD**) was synthesized, and a highly selective glucagon sensor, **Glucagon Yellow (BD-105)**, was discovered by fluorescence image-based screening method. **BD** library was synthesized via a Knoevenagel-type condensation reaction with 160 benzaldehydes and the 1,3 dimethyl-BODIPY scaffold. Using **BD** compounds, a fluorescence image-based screening was performed against three cell lines including AlphaTC1 and BetaTC6 cells which secrete glucagon and insulin, respectively, and HeLa as control cells. Out of the 160 candidate probes, one compound, **Glucagon Yellow**, exhibited selective staining only in AlphaTC1 cells. The selectivity of **Glucagon Yellow** toward glucagon was confirmed *in vitro* by comparison of its fluorescence intensity change against 19 biologically relevant analytes. Subsequent immunostaining experiments revealed that **Glucagon Yellow** and the glucagon antibody colocalized in pancreas tissue, showing a high quantitative correlation analysis by the *Pearson's coefficient constant* ($R_r = 0.950$). These results demonstrated the potential application of **Glucagon Yellow** as a glucagon imaging agent in live cells and tissues.

Introduction

Fluorescent small molecules have been widely used for sensors and bioimaging probes.¹ Most fluorescent probes have been developed on a case-by-case basis by connecting a recognition motif to a fluorophore.² While there are many successful cases reported, the conventional approach usually limits the scope of the probes to known binding motifs or fluorophores. As an alternative approach, our research group has pursued a diversity-oriented fluorescence library approach (DOFLA) and demonstrated the generality of this approach by developing sensors and bioimaging agents for various targets, including DNA,³ RNA,^{4,5} β -amyloid,^{6,7} GTP,⁸ heparin,⁹ chy-

motrypsin,¹⁰ human serum albumin (HSA),¹¹ glutathione,¹² and myotube cell state.¹³ On the basis of the successful experience with the previous fluorophore library, we are expanding this DOFLA concept to a superior fluorophore, 4,4-difluoro-4-bora-3a,4a-diaza-s-indacene (BODIPY) to develop high performance imaging probes.

BODIPY has outstanding photophysical properties as a fluorescent scaffold, such as high photostability, high fluorescent quantum yield, high extinction coefficient, and narrow emission bandwidth.¹⁴ The chemical modification of the BODIPY scaffold has been well studied.¹⁵ However, a systematic construction of a library based on BODIPY has not been reported yet, maybe

[†] Department of Chemistry, New York University.

[‡] Department of Chemistry, National University of Singapore.

[§] MedChem Program of Life Sciences Institute, National University of Singapore.

[‡] Laboratory of Bioimaging Probe Development, Singapore Bioimaging Consortium, Agency for Science, Technology and Research (ASTAR).

(1) Que, E. L.; Domaille, D. W.; Chang, C. J. *Chem. Rev.* **2008**, *108*, 1517–1549.

(2) (a) deSilva, A. P.; Gunaratne, H. Q. N.; Gunnlaugsson, T.; Huxley, A. J. M.; McCoy, C. P.; Rademacher, J. T.; Rice, T. E. *Chem. Rev.* **1997**, *97*, 1515–1566. (b) Martinez-Manez, R.; Sancenon, F. *Chem. Rev.* **2003**, *103*, 4419–4476.

(3) Lee, J. W.; Jung, M.; Rosania, G. R.; Chang, Y. T. *Chem. Commun.* **2003**, 1852–1853.

(4) Li, Q.; Chang, Y. T. *Nat. Protoc.* **2006**, *1*, 2922–2932.

(5) Li, Q.; Kim, Y.; Namm, J.; Kulkarni, A.; Rosania, G. R.; Ahn, Y. H.; Chang, Y. T. *Chem. Biol.* **2006**, *13*, 615–623.

(6) Li, Q.; Lee, J. S.; Ha, C.; Park, C. B.; Yang, G.; Gan, W. B.; Chang, Y. T. *Angew. Chem., Int. Ed.* **2004**, *43*, 6331–6335.

(7) Li, Q.; Min, J.; Ahn, Y. H.; Namm, J.; Kim, E. M.; Lui, R.; Kim, H. Y.; Ji, Y.; Wu, H.; Wisniewski, T.; Chang, Y. T. *ChemBioChem* **2007**, *8*, 1679–1687.

(8) Wang, S.; Chang, Y. T. *J. Am. Chem. Soc.* **2006**, *128*, 10380–10381.

(9) Wang, S.; Chang, Y. T. *Chem. Commun.* **2008**, 1173–1175.

(10) Wang, S.; Kim, Y. K.; Chang, Y. T. *J. Comb. Chem.* **2008**, *10*, 460–465.

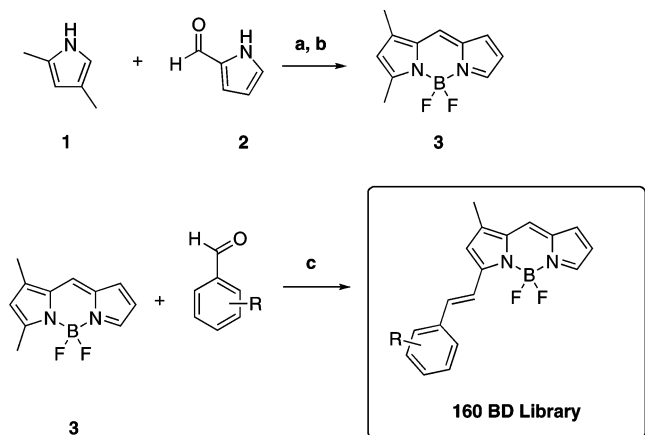
(11) (a) Min, J.; Lee, J. W.; Ahn, Y. H.; Chang, Y. T. *J. Comb. Chem.* **2007**, *9*, 1079–1083. (b) Ahn, Y. H.; Lee, J. S.; Chang, Y. T. *J. Comb. Chem.* **2008**, *10*, 376–380.

(12) Ahn, Y. H.; Lee, J. S.; Chang, Y. T. *J. Am. Chem. Soc.* **2007**, *129*, 4510–4511.

(13) Wagner, B. K.; Carrinski, H. A.; Ahn, Y. H.; Kim, Y. K.; Gilbert, T. J.; Fomina, D. A.; Schreiber, S. L.; Chang, Y. T.; Clemons, P. A. *J. Am. Chem. Soc.* **2008**, *130*, 4208–4209.

(14) Karolin, J.; Johansson, L. B. A.; Strandberg, L.; Ny, T. *J. Am. Chem. Soc.* **1994**, *116*, 7801–7806.

(15) (a) Loudet, A.; Burgess, K. *Chem. Rev.* **2007**, *107*, 4891–4932. (b) Ulrich, G.; Ziessel, R.; Harriman, A. *Angew. Chem., Int. Ed.* **2008**, *47*, 1184–1201.

Scheme 1. Synthesis of BD Library^a

^a Reagents and conditions: (a) POCl_3 , dichloromethane, -5°C for 3 h, then 3 h at rt; (b) $\text{BF}_3 \cdot \text{OEt}_2$, DIEA, rt for 3 h (overall yield: 51%); (c) R-CHO (160 aromatic aldehydes, see Table S1, Supporting Information), pyrrolidine, AcOH, EtOH, microwave irradiation, 2–15 min.

due to the synthetic challenges.¹⁶ Here, we report the synthesis of the first BODIPY-based library, and the subsequent discovery of a glucagon sensor.

Glucagon is an important hormone peptide involved in carbohydrate metabolism. It is produced by alpha cells in the pancreas and maintains the level of glucose in the blood by effects opposite to those of insulin.¹⁷ Glucagon release in alpha cells is normally stimulated as the concentration of glucose in the blood decreases, a response that is progressively diminished in type 1 diabetes.¹⁸

Although there have been extensive biological studies about glucagon secretion and its related diseases such as diabetes, there are no small-molecule fluorescent probes to visualize glucagon to date. Therefore, the development of fluorescent probes that could quantify the concentration of glucagon in live cells or tissues would be of great importance.

Results and Discussion

Design and Synthesis of a BODIPY Library. In order to introduce systematic structural diversity on the BODIPY scaffold, we designed a synthetic scheme to append different styryl motifs to the BODIPY fluorophore. Styryl-derivatized BODIPY compounds are known to display red-shifted fluorescence emissions due to the extended π -conjugation,¹⁹ and their emission wavelengths vary according to the styryl domain. Since hundreds of aldehyde building blocks are commercially available, styryl-containing BODIPY compounds constitute a feasible target for combinatorial library synthesis. While the syntheses of both monostyryl and distyryl compounds have been reported from symmetric tetramethyl-BODIPY intermediates, the isolation of the two possible condensation products would make difficult the construction of a library.¹⁹ Therefore, in order to make easier such complex purification procedures, we synthesized 1,3-dimethyl-BODIPY scaffold (3), which can only lead to the monostyryl products. Compound 3 was prepared by condensation of pyrrole-2-carboxaldehyde and 2,4-dimethylpyrrole at low temperature, followed by the addition of $\text{BF}_3 \cdot \text{OEt}_2$.²⁰ Second, the monostyryl-containing BODIPY library (named **BD**) was constructed using 238 aromatic aldehydes via Knoevenagel condensation under microwave irradiation, purify-

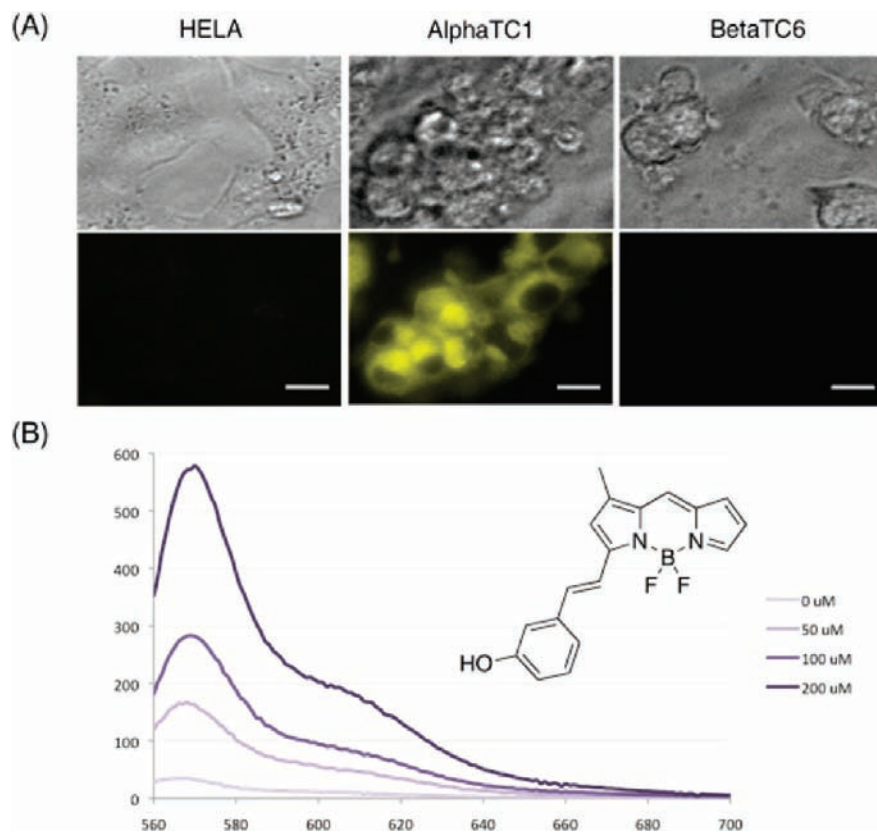


Figure 1. (A) Fluorescence microscope images of **BD-105** in three different cell lines. Cells were stained with the compound at 500 nM for 24 h. Upper row corresponds to the bright-field images, and the lower row illustrates the fluorescence images (TRITC channel: excitation 540 nm, emission 580 nm). Scale bar: 20 μm (B) *In vitro* fluorescence responses of **BD-105** (1 μM) toward glucagon. Spectra obtained in 10 mM HEPES (pH 7.4) with excitation at 530 nm.

In vitro fluorescence response of BD-105

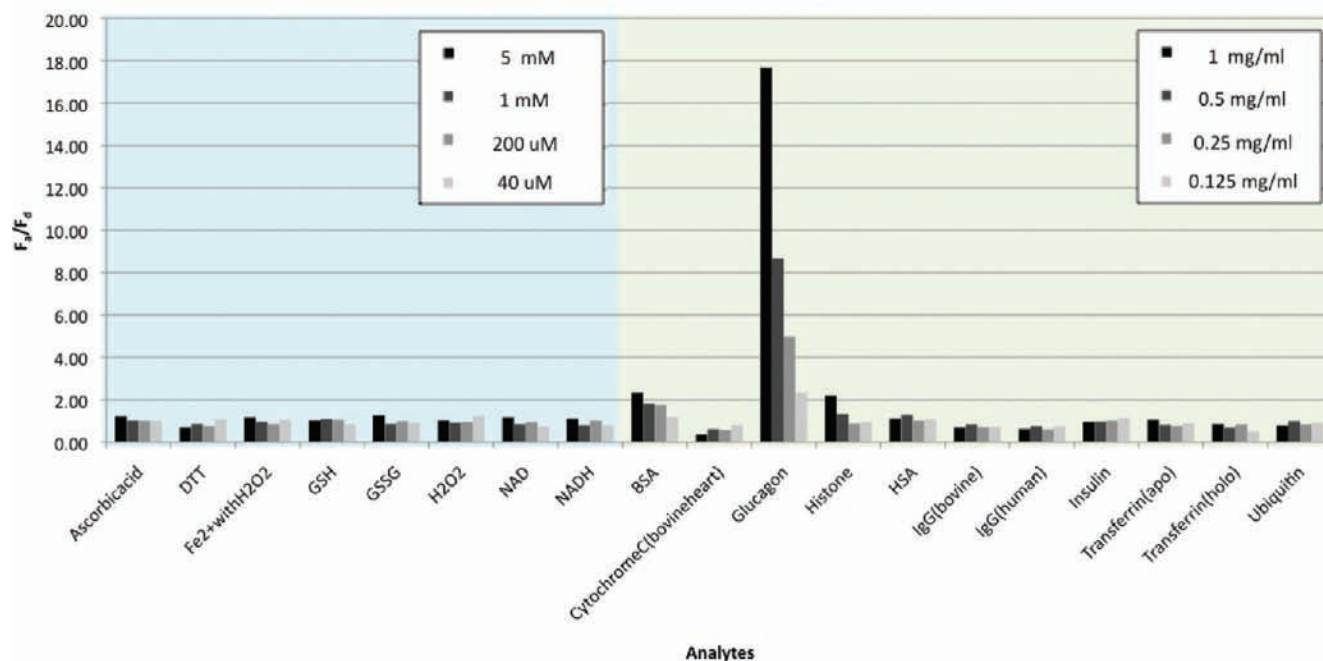


Figure 2. Fluorescence response of **BD-105** toward a series of analytes. The intensities of **BD-105** in the presence of each analyte (F_a) were compared with fluorescence intensities of **BD-105** (F_d) in 10 mM HEPES buffer (pH 7.4). Bars represent the ratio of F_a/F_d . The concentration of small-molecule analytes (blue background) ranged from 40 μ M to 5 mM, and that of macromolecule analytes (green background) from 0.125 mg/mL to 1 mg/mL.

ing the final products by semi-preparative RP-HPLC (Scheme 1). After HPLC–MS characterization, 160 compounds were collected for further studies (average purity 96.5% at 250 nm, Table S2, Supporting Information).

Spectroscopic Properties. The spectroscopic properties of the **BD** compounds are summarized in Table S2 Supporting Information. All library compounds exhibited red-shifted fluorescence emissions compared to **3** ($\lambda_{em} = 512$ nm). Their spectroscopic properties are diverse, with maximum absorption wavelengths ranging from 525 to 605 nm, and maximum emission wavelengths from 560 to 730 nm. **BD** compounds displayed relatively low fluorescence quantum yields compared to **3**, with an average value of 0.32, which maybe due to their higher structural flexibility. These findings suggest that many of the **BD** compounds could be used not only as fluorescent quenching sensors but also as fluorescent turn-on sensors.

Image-Based Screening in Live Cells. Based on our previous experience,⁵ the successful discovery of novel imaging probes is highly dependent on both the chemical diversity of the fluorescence library and the screening methodology. Regarding the screening methods, two opposite approaches can be used: target-to-system and system-to-target. Target-to-system approaches utilize high-throughput *in vitro* screening techniques to find probes, which undergo fluorescence property changes upon interaction with a certain analyte. After a primary selection, successful candidates are further validated for biologically relevant applications.^{7,12} On the other hand, system-to-target approaches initially screen collections of fluorophores in complex biological systems, and further investigate the origin of their fluorescence response in a forward chemical genetics manner. For example, imaging agents of DNA and RNA were discovered after *in vitro* screening a series of nucleus- or nucleolus-staining primary hits against DNA and RNA, respectively.^{3,5} Because the intrinsic cellular localization of the fluorophores may allow their specific interaction with some

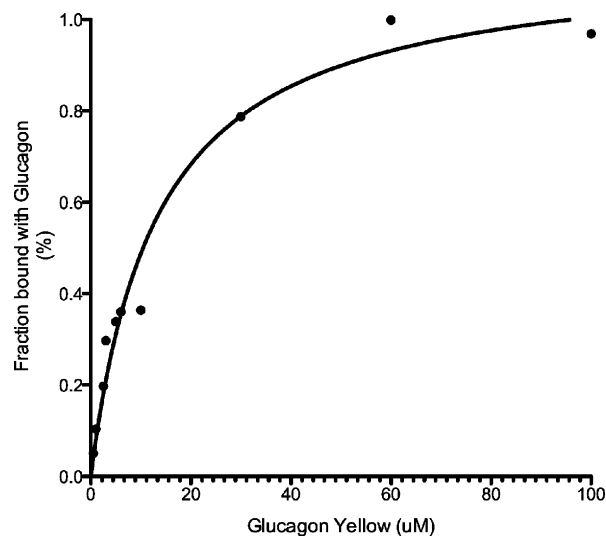


Figure 3. Fractional saturation curve of **Glucagon Yellow** vs glucagon. Various concentrations of **Glucagon Yellow** were incubated with 2 μ M glucagon for 30 min at rt, followed by the measurement of the fluorescence emission. Experimental $K_D = 13.3$ μ M.

biomolecules, this approach can minimize the number of false positive hits and accelerate the overall probe discovery process.¹³

Cell permeability and reasonable fluorescent quantum yields are critical requirements for the application of system-wide cell image-based screenings. Nonpermeable probes or significantly dimmed fluorophores are not practical tools, as they need a large amount of compound, which may induce some cytotoxic effects. Having determined a reasonable fluorescence quantum yield for the **BD** compounds, we tested their cell permeability in 3T3-L1 and HeLa cells. Most of the **BD** library members showed good cell permeability (data not shown), as many previously reported BODIPY probes,²¹ and the **BD** library was proven to fulfill the requirements

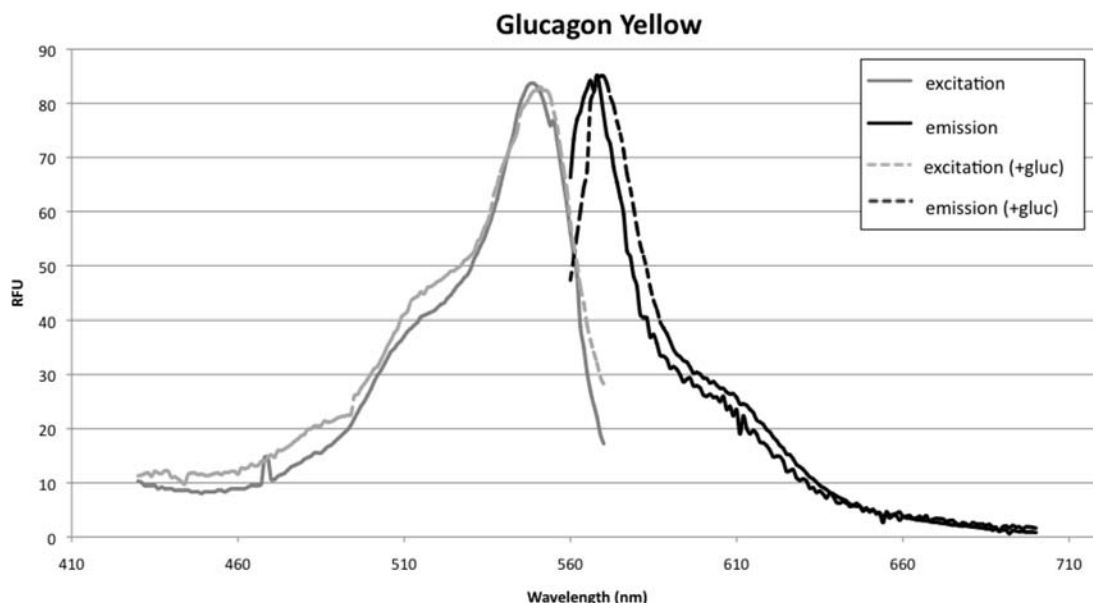


Figure 4. Normalized fluorescence excitation and emission spectrum of **Glucagon Yellow** ($10 \mu\text{M}$), before and after binding to glucagon. Before addition of glucagon: absorption λ_{max} 550 nm, emission λ_{max} 568 nm; upon binding to glucagon: absorption λ_{max} 553 nm, emission λ_{max} 570 nm. All experiments were performed in 10 mM HEPES buffer (pH 7.4).

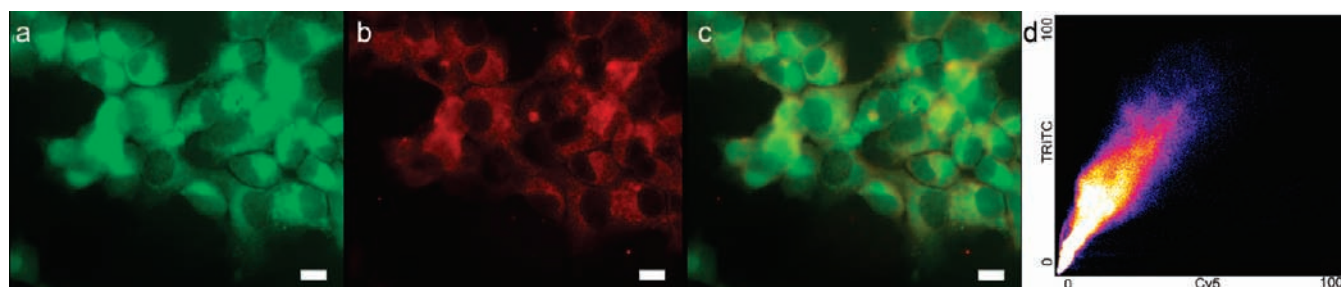


Figure 5. Fluorescence colocalization images of **Glucagon Yellow** in AlphaTC1 cells. Fluorescence microscope images of **Glucagon Yellow** (a: TRITC channel), glucagon antibody (b: Cy5 channel), and merged images (c). Colocalization scatter plot (d: Pearson's coefficient 0.896). Scale bar $20 \mu\text{m}$.

for cell-based fluorescence image evaluation. **BD** compounds were screened toward three distinct cell lines as hormone peptide sensors. We selected AlphaTC1, BetaTC6, which respectively secrete glucagon and insulin,²² and HeLa cells as a control. All the compounds were tested by image-based high-throughput screening, and fluorescence images were taken at different incubation times. Bright field images were also taken to ensure cell viability. Notably, after 24 h incubation **BD-105** exhibited a selective and high fluorescent intensity in AlphaTC1, which is a glucagon secreting cell line, compared to BetaTC6 or HeLa cells (Figure 1 A), indicating its potential selective fluorescence increase upon interaction with glucagon.

In Vitro Fluorescence Response. After *in vitro* experiments indicated a strong fluorescence increase (up to 17-fold) of **BD-105** upon treatment with glucagon (Figure 1-B), we proceeded to evaluate its selectivity by screening the compound against a set of 18 biologically relevant analytes. **BD-105** displayed an impressive selectivity toward glucagon compared to serum albumins (both BSA and HSA, common nonselective hydrophobic fluorescence increasing proteins, Figure 2) and insulin, the counter-regulatory hormone (Figure S3, Supporting Information). On the basis of its selectivity pattern and visual yellow fluorescence color, we decided to name **BD-105** as “**Glucagon Yellow**”.

Fluorescence Titration and Spectroscopic Change by Binding to Glucagon. To further investigate the binding properties of **Glucagon Yellow**, various concentrations of **Glucagon**

Yellow were titrated with glucagon peptide. Fractional saturation curve of **Glucagon Yellow** with glucagon revealed a dissociation constant (K_D) of $13.3 \mu\text{M}$ (Figure 3). **Glucagon Yellow** ($1 \mu\text{M}$) displayed a weak fluorescence emission ($QY = 0.012$) in 10 mM HEPES buffer (pH 7.4), with an absorption maximum at 550 nm and an emission maximum of 568 nm (Figure 4). Upon addition of glucagon ($200 \mu\text{M}$) to the solution, a marked increase of the fluorescence intensity was observed ($QY = 0.151$), with a slight red-shifted absorption (553 nm) and emission (570 nm) maxima.

Immuno-Staining of Glucagon in AlphaTC1 cell and Pancreatic Tissue. To validate the biological relevance of **Glucagon Yellow** as a glucagon-imaging agent, we further compared the staining pattern of the probe with a fluorescently labeled glucagon antibody. **Glucagon Yellow** proved to colocalize with a glucagon antibody, both in the AlphaTC1 cells and in mouse pancreas tissue sections, with a high linearity in their colocalization scatter plot (Figures 5 and 6). The quantitative colocalization analysis demonstrated that the fluorescence signals from **Glucagon Yellow** and the glucagon antibody showed a positive correlation with a high *Pearson's coefficient* (Pearson's coefficient ranges from -1 to 1 . Values close to 1 indicate a reliable colocalization) ($R_r = 0.950$) from the pancreas tissue.²³ Additionally, the staining pattern of **Glucagon Yellow** differed from that of insulin antibody image, demonstrating the clear selectivity

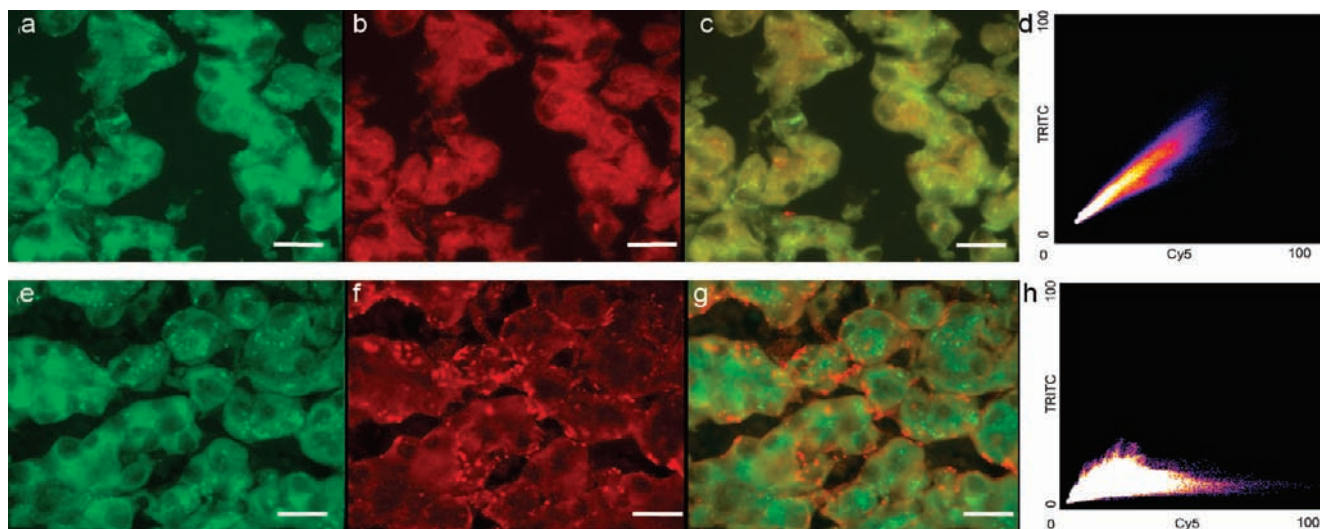


Figure 6. Fluorescence colocalization images of **Glucagon Yellow** in pancreas tissue. Fluorescence microscope images of **Glucagon Yellow** (a, e: TRITC channel), glucagon antibody (b: Cy5 channel), insulin antibody (f: Cy5 channel) and merged images (c for a plus b, g for e plus f). Colocalization scatter plot (d: Pearson's coefficient 0.950, h: Pearson's coefficient 0.681). Scale bar 20 μm .

of this probe to glucagon in both AlphaTC1 cells and pancreas tissue (Figure 6g).

Conclusion

We have synthesized the first BODIPY library (**BD** library) as potential bioimaging probe toolbox, and discovered the first live cell/tissue glucagon fluorescent probe. One hundred and sixty **BD** compounds were prepared by condensation with a series of aldehydes, and a diverse range of the spectroscopic properties for the final compounds was observed. By means of a fluorescence image-based screening against three cell-lines, we identified a unique imaging probe, **Glucagon Yellow**, capable to selectively stain AlphaTC1 cells. Further experiments indicated a selective fluorescence emission increase upon interaction of glucagon. Immunostaining experiments demonstrated that **Glucagon Yellow** colocalizes selectively with glucagon antibody not only in AlphaTC1 cells but also in pancreas tissue. This is the first example of a small-molecule fluorescent probe that can be used to visualize glucagon in live cells, representing a useful imaging probe for biological studies of glucagon secretion and glucagon-related diseases.

Experimental Section

Materials and Methods. All the materials were obtained from commercial suppliers (Acros and Aldrich) and used without further

purification. Aldehyde building blocks were purchased from Aldrich, Acros, and Maybridge Inc. Normal phase chromatography of the intermediates was performed using Merck Silica Gel 60 (particle size: 0.040–0.063 mm, 230–400 mesh ASTM), and the solvents used for the spectroscopy experiments were of spectrophotometric grade. All library compounds were purified in a semipreparative Gilson RP-HPLC using a C18 column (100 mm \times 21.2 mm, Axia column from Phenomenex Inc.). LC-MS characterization was performed on a LC-MS-IT-TOF Prominence Shimadzu Technology, using a DAD (SPD-M20A) detector, and a C18 column (20 mm \times 4.0 mm, 100 \AA , Phenomenex Inc.), with 4 min elution using a gradient solution of $\text{CH}_3\text{CN-H}_2\text{O}$ (containing 0.1% TFA) and an electrospray ionization source. ^1H and ^{13}C NMR spectra were recorded on a Bruker Avance 300 NMR spectrometer.

1,3-Dimethyl 4,4-Difluoro-4-bora-3a,4a-diaza-s-indacene (1,3-Dimethyl-BODIPY, 3). Pyrrole 2-carboxyaldehyde (300 mg, 3.15 mmol) was dissolved in absolute dichloromethane (4 mL) and cooled down to -5°C under nitrogen atmosphere. 2,4-dimethylpyrrole (324.6 μL , 3.15 mmol) was added to the reaction mixture and stirred for 3 min, followed by slow dropwise addition of POCl_3 (288.3 μL , 3.15 mmol). The reaction mixture was stirred at -5°C for 3 h, then another 3 h at rt. Once the starting materials were consumed following TLC monitoring, 1.5 mL (9.45 mmol) of diisopropylethylamine (DIEA) and 1.2 mL (9.45 mmol) of BF_3OEt_2 were added. After 3 h, the reaction mixture was washed with H_2O ($\times 3$) and dried over Na_2SO_4 . The solvent was evaporated, and the residue was purified by silica gel column chromatography (hexane/EtOAc = 5:1) to yield 227.2 mg (1.03 mmol, 32.8%) of **3** as a red solid product. ^1H NMR (300 MHz, CDCl_3) δ 2.28 (s, 3H), 2.59 (s, 3H), 6.16 (s, 1H), 6.43 (s, 1H), 6.93 (s, 1H), 7.20 (s, 1H), 7.64 (s, 1H). ESI-MS m/z (M^+) calc: 220.10, found: 243.10 ($\text{M} + \text{Na}$).

General Procedure for the Aldehyde Condensation Reaction. *Method 1* (for aromatic aldehydes containing phenol moieties): **3** (15 mg, 68 μmol) and aldehyde (68 μmol , 1 equiv) (Table S1) were dissolved in absolute EtOH, with 10 equiv of pyrrolidine (48 μL , 680 μmol) and 10 equiv of AcOH (35 μL , 680 μmol). The condensation reaction was performed by using consecutive 1 min-

- (16) Lavis, L. D.; Raines, R. T. *ACS Chem. Biol.* **2008**, *3*, 142–155.
 (17) (a) Gelling, R. W.; Du, X. Q.; Dichmann, D. S.; Romer, J.; Huang, H.; Cui, L.; Obici, S.; Tang, B.; Holst, J. J.; Fledelius, C.; Johansen, P. B.; Rossetti, L.; Jelicks, L. A.; Serup, P.; Nishimura, E.; Charon, M. J. *Proc. Natl. Acad. Sci. U.S.A.* **2003**, *100*, 1438–1443. (b) Ravier, M. A.; Rutter, G. A. *Diabetes* **2005**, *54*, 1789–1797.
 (18) Gerich, J. E.; Langlois, M.; Noacco, C.; Karam, J. H.; Forsham, P. H. *Science* **1973**, *182*, 171–173.
 (19) (a) Baruah, M.; Qin, W.; Flors, C.; Hofkens, J.; Vallee, R. A.; Beljonne, D.; Van der Auweraer, M.; De Borggraeve, W. M.; Boens, N. *J. Phys. Chem. A* **2006**, *110*, 5998–6009. (b) Atilgan, S.; Ozdemir, T.; Akkaya, E. U. *Org. Lett.* **2008**, *10*, 4065–4067.
 (20) Wu, L.; Burgess, K. *Chem. Commun.* **2008**, 4933–4935.
 (21) (a) Verdoes, M.; Hillaert, U.; Florea, B. I.; Sae-Heng, M.; Risseeuw, M. D. P.; Filippov, D. V.; Van der Marel, G. A.; Overkleeft, H. S. *Bioorg. Med. Chem. Lett.* **2007**, *17*, 6169–6171. (b) Yee, M.; Fas, S. C.; Stohlmeyer, M. M.; Wandless, T. J.; Cimprich, K. A. *J. Biol. Chem.* **2005**, *280*, 29053–29059. (c) Verdoes, M.; et al. *Chem. Biol.* **2006**, *13*, 1217–1226. (d) Domaille, D. W.; Que, E. L.; Chang, C. J. *Nat. Chem. Biol.* **2008**, *4*, 168–175.

- (22) (a) Powers, A. C.; Efrat, S.; Mojsov, S.; Spector, D.; Habener, J. F.; Hanahan, D. *Diabetes* **1990**, *39*, 406–414. (b) Poitout, V.; Stout, L. E.; Armstrong, M. B.; Walseth, T. F.; Sorenson, R. L.; Robertson, R. P. *Diabetes* **1995**, *44*, 306–313.
 (23) (a) Li, Q.; Lau, A.; Morris, T. J.; Guo, L.; Fordyce, C. B.; Stanley, E. F. *J. Neurosci.* **2004**, *24*, 4070–4081. (b) Manders, E. M. M.; Verbeek, F. J.; Aten, J. A. *J. Microsc.* **1993**, *169*, 375–382.

step microwave irradiation (700 W). After every step, the reaction mixture was cooled down to rt and then monitored by TLC. The reactions were finished between 5 to 20 min. The resulting crude mixtures were concentrated under vacuum, and purified by semipreparative RP-HPLC. Combined purification fractions were dried using a GeneVac evaporator. *Method 2* (for rest of aromatic aldehydes): **3** (15 mg, 68 μ mol) and aldehyde (68 μ mol, 1 equiv) (Table S1, Supporting Information) were dissolved in absolute EtOH, with 10 equiv of pyrrolidine (48 μ L). The condensation reaction was performed by using consecutive 1 min-step microwave irradiation (700 W). After every step, the reaction mixture was cooled down to rt, and then monitored by TLC. The reactions were finished between 5 to 20 min. The resulting crude mixtures were concentrated under vacuum and purified by semipreparative RP-HPLC. Combined purification fractions were dried using a GeneVac evaporator.

Characterization of BD-Library. All the library compounds were characterized by LC-MS (See Table S2, Supporting Information).

Characterization of Glucagon Yellow (BD-105): ^1H NMR (300 MHz, DMSO- d_6) δ 2.35 (s, 3H) 6.51 (dd, $J = 1.80, 3.72$ Hz, 1H) 6.82 (m, 1H) 7.02–7.14 (m, 4H) 7.26 (t, $J = 7.71$ Hz, 1H) 7.37 (d, $J = 16.4$ Hz, 1H, C=CH trans) 7.70 (d, $J = 16.3$ Hz, 1H, C=CH trans) 7.71 (s, 1H) 7.80 (s, 1H) 9.66 (s, 1H), ^{13}C NMR (75.5 MHz, DMSO- d_6) δ 11.56, 113.58, 116.99, 117.66, 117.97, 118.16, 119.55, 125.32, 127.04, 130.62, 133.34, 137.18, 137.72, 139.16, 141.20, 145.85, 158.25, 158.48, ESI-MS (m/z) calcd: 324.10 found 325.10 (M + H).

Quantum Yield Measurements. Quantum yields were calculated by measuring the integrated emission area of the fluorescent spectra and comparing that value to the area measured for rhodamine B in EtOH when excited at 500 nm ($\Phi_{\text{rho-B}} = 0.70$). Quantum yields for the BD library were then calculated using eq 1, where F represents the area of fluorescent emission, n is reflective index of the solvent, and Abs is absorbance at excitation wavelength selected for standards and samples. Emission was integrated between 530 to 700 nm.

$$\Phi_{\text{flu}}^{\text{sample}} = \Phi_{\text{fl}}^{\text{reference}} \left(\frac{F^{\text{sample}}}{F^{\text{reference}}} \right) \left(\frac{\eta^{\text{sample}}}{\eta^{\text{reference}}} \right) \left(\frac{\text{Abs}^{\text{reference}}}{\text{Abs}^{\text{sample}}} \right) \quad (1)$$

In Vitro Fluorescence Screening. BD-105 (10 μ M) was evaluated in 10 mM HEPES, pH 7.4. Fluorescence intensities were measured using a Spectra Max Gemini XSF plate reader in 384-well format. Excitation was provided at 530 nm, and emission was obtained starting from 560 to 630 nm. All the analytes were tested at four serial concentrations: macromolecule analytes ranged from 0.125 mg/mL to 1 mg/mL (BSA, HSA, cytochrome C (bovine heart), glucagon, histone, IgG(bovine), IgG(human), insulin, transferrin(apo), transferrin(holo), ubiquitin), and concentrations of small-molecule analytes varied from 40 μ M to 1 mM (DTT, GSH, GSSG, H_2O_2 , NAD, NADH, ascorbic acid).

Determination of the Dissociation Constant for Glucagon Yellow to Glucagons. The fluorescent emission spectra of glucagon with various concentrations of **Glucagon Yellow** were measured on a SpectraMax M2 plate reader. The fluorescent titration curve was fitted to the standard equation using Graphpad Prism v5

software. Glucagon (2 μ M) solution was titrated by different concentrations of **Glucagon Yellow** (0.5–100 μ M), and the fluorescence intensities were measured at 568 nm with (excitation: 520 nm). The bound fraction (X) of **Glucagon Yellow** at each concentration was determined using the eq 2

$$X = \frac{F_c - F_o}{F_{\text{sat}} - F_o} \quad (2)$$

where F_c and F_o are the fluorescence intensities of a given concentration of **Glucagon Yellow** with and without glucagon, respectively. F_{sat} is the fluorescence intensity at the same concentration of Glucagon Yellow when fully bound. F_{sat} was determined by fluorescence titration at each concentration with a series concentration of glucagon. The results were plotted according to nonlinear fitting curve eq 3

$$F = F_o + (F_{\text{sat}} - F_o) \frac{[GY]}{K_D + [GY]} \quad (3)$$

where K_D is the dissociation constant, $[GY]$ is the concentration of **Glucagon Yellow**.

Cell Culture. 3T3-L1 and HELA cells were grown in Dulbecco's Modified Eagle Medium (DMEM, GIBCO) supplemented with 10% fetal bovine serum (FBS) and antibiotics (100 μ g/mL penicillin/streptomycin mixture) in a humidified atmosphere at 37 $^\circ\text{C}$ with 5% CO_2 . AlphaTC1 Clone 9 (ATCC) were grown in Dulbecco's Modified Eagle's Medium (DMEM, GIBCO) with 4 mM L-glutamine, 3.0 g/L glucose, 1.5 g/L sodium bicarbonate, and 10% heat-inactivated dialyzed fetal bovine serum in a humidified atmosphere at 37 $^\circ\text{C}$ with 5% CO_2 . Beta-TC-6 (ATCC) cells were grown in Dulbecco's Modified Eagle's medium (DMEM, GIBCO) with 15% heat-inactivated fetal bovine serum in a humidified atmosphere at 37 $^\circ\text{C}$ with 5% CO_2 .

Immunohistochemistry (Frozen Mouse Pancreas). Mouse pancreas was cut into smaller pieces (~5 mm long) with a razor blade, and 10 μ m sections were cut on a MICROM/HM520. Sections were used within one week of cutting. Before staining, the sections were fixed with cold acetone for 10 min. Immunohistochemistry images of frozen sections with the anti-glucagon monoclonal antibody and **Glucagon Yellow** were obtained from NIKON T1 fluorescence microscopy (540/580 nm filter-TRITC channel for **Glucagon Yellow** and Cy5 filter (650/680 nm) for glucagon antibody visualization).

Acknowledgment. We gratefully acknowledge National University of Singapore (NUS) for the financial support (Young Investigator Award: R-143-000-353-123). J.S.L. was supported by a Korea Research Foundation Grant funded by the Korean government (MOEHRD, Basic Research Promotion Fund: KRF-2005-C00088).

Supporting Information Available: Complete ref 21c; HPLC data and chemical structures for the 160 **BD** compounds. This material is available free of charge via the Internet at <http://pubs.acs.org>.

JA9011657